

HYDRODYNAMICS MODELING OF PARTICULATES COATING IN A FLUIDIZED BED

Vahid Abdolkarimi

Department of process and equipment technology development, Research Institute of Petroleum Industry, 1485733111, Tehran, Iran, v.abdolkarimi@gmail.com

Received January 24, 2014, Accepted March 10, 2014

Abstract

A Computational Fluid Dynamics model based on Eulerian formulation for multiphase flow is presented to model the hydrodynamics of particulates motion in a conic fluidized bed in presence of pneumatic nozzle jet flow. The velocity profile of outlet gas from nozzle in fluidized bed is similar to free jet velocity profile and is obtained from Schlichting equation. The static pressure of gas-solid mixture, velocity distribution of gas and solid particles and the particles volume fraction distribution in the bed are considered. For validation of Computational model, the predicted height of fluidized particles bed is compared with similar experimental published data which indicates good agreement.

Keyword: CFD; Eulerian model; Fluidized bed; Hydrodynamics.

1. Introduction

Fluidized bed coating is vastly used in pharmaceutical and food industries to increase the life time of active ingredients, to cover the odor or taste of materials, to control the releasing of active pharmaceutical components inside human body or to facilitate the transportation of materials [1]. Fluidized bed coating consists of three major steps [2]:

- 1) Fluidizing solid particles.
- 2) Atomizing coating solution on the bed of fluidized particles.
- 3) Drying the coated particles to evaporate the solvent of coating solution.

The atomized droplets consist of solute which acts as a covering layer and solvent which coating material is solved in it or forms a slurry solution with coating material. When liquid droplets contact solid particles they spread over the surface of particles. The fluidizing gas evaporates the solvent and leaves a layer of coating material on particles surface. Particles growth is usually occurred by two mechanisms,

- 1) the agglomeration of fine particles due to liquid bridge between two or more smaller particles, this process is happened when the liquid bridge is strong enough to hold particles together and
- 2) the growth of coating layer on a particle [2].

There are numerous variables that influence a fluidized bed coating process and a thorough insight into their action is essential for establishing an appropriate thermodynamic operation point that provides the required process and product quality. The key variables in fluidized bed coating are indicated in table 1 [2]. These variables are divided in to three categories: process variables, design variables and physical property variables (physical properties of coating material and solid particles). According to Schlunder and Link [3], at the moment, trial and error is the only way to determine optimum operating conditions in fluidized bed coating process. This is due to enormous number of variables that affect fluidized bed coating process, fast process kinetic, different local conditions inside a fluidized bed [4], recirculation of fluidizing gas and particles bypass around the coating zone.

In this research the Computational fluid dynamic (CFD) modeling of particles hydrodynamics in fluidized bed in presence of nozzle air flow is performed and contours of gas and solid velocity, solid volume fraction and mixture static pressure are calculated. CFD modeling can be used

to investigate the effect of different variables on fluidized bed coating process. By use of CFD model it is possible to define flexible model for different operating conditions and determine optimum conditions.

Table1 Key variables in fluidized bed coating process [2]

Fluidization	Drying air flow rate Equipment type and dimensions Substrate size, size distribution, density Substrate surface character (charge or chemical composition) Batch size
Atomization	Spray mode (top, bottom, etc.) Droplet size Nozzle design (pneumatic, ultrasonic, rotary) Nozzle distance from bed Atomizing air flow rate (pneumatic) Coating spray rate Coating solution viscosity, surface tension, density
Drying	Inlet temperature Drying air flow rate Outlet air relative humidity Liquid coating concentration Atomizing air flow rate

2. Experimental setup

The experimental validation setup is depicted in figure1. The tapered reactor had a bottom diameter of 0.225 m, a top diameter of 0.45 m, and a total height of 0.84 m. Fluidization air was provided by a 2.2 kW high-pressure centrifugal fan. The air distributor consisted of a Robusta 172×36 wpi wire mesh. A pneumatic nozzle (Schlick Model 970-S1, Untersiemau, Germany) was installed at the tip of a retractable rod, allowing adjustable nozzle height. The nozzle’s air volumetric flow rate \dot{V}_{at} (in Nm³s⁻¹), was obtained through measuring the linear air velocity with a Testo 0.1m diameter anemometer (Testo, Ternat, Belgium) while blowing compressed dry air through the nozzle at different atomization pressures (0.5, 1.0, 1.5, 2.0, 2.5, 3.0, 3.5, and 4 bar) in a cylindrical pipe with a diameter of 0.1m and a length of 0.5 m. Regression analysis resulted in the following correlation between P_{at} and \dot{V}_{at} [5]:

$$\dot{V}_{at} = -10^{-4} P_{at}^2 + 1.3873 \times 10^{-3} P_{at} + 1.7867 \times 10^{-3} \quad (1)$$

Micropearl glass beads (Sovitec, Fleurus, Belgium) with $d_{43}=365 \mu\text{m}$ were used as the core material.

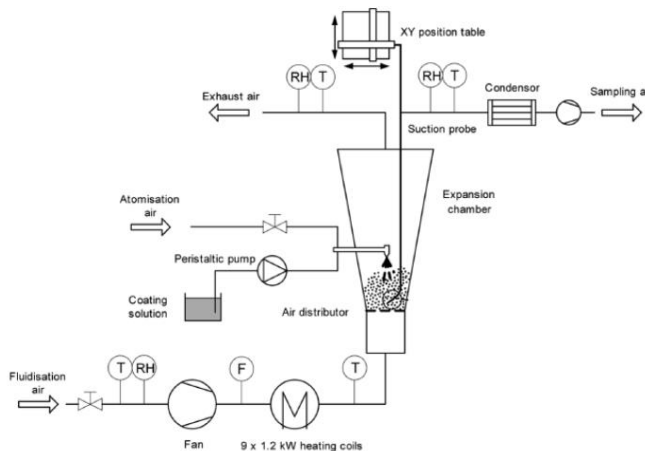


Figure1. Experimental validation setup [5]

3. Mathematical model

CFD modeling involves three main steps: (1) Creating the model geometry and grid. (2) Defining the appropriate physical models and (3) Defining the boundary and operating conditions. The governing conservation equations of mass, momentum and physical models involved in the process are discretized over control volumes and solved by finite volume method.

The generated 2D-grid for experimental geometry is depicted in figure2. Solid-gas flow modeling is performed in Eulerian framework which considers gas and solid particles as two continuum phases that penetrate in each other. The contribution of each phase in conservation equations is determined by its volume fraction. Solid particles are treated as granular flow which is a model on the basis of gas molecules motion. In this study only the hydrodynamics of solid-gas flow inside a fluidized bed in presence of nozzle jet flow is considered.

The continuity equation for each phase is:

$$\frac{\partial(\alpha_k \rho_k)}{\partial t} + \nabla \cdot (\alpha_k \rho_k \vec{U}_k) = 0 \quad (2)$$

where \vec{U}_k is the velocity and α_k is the volume fraction of each phase.

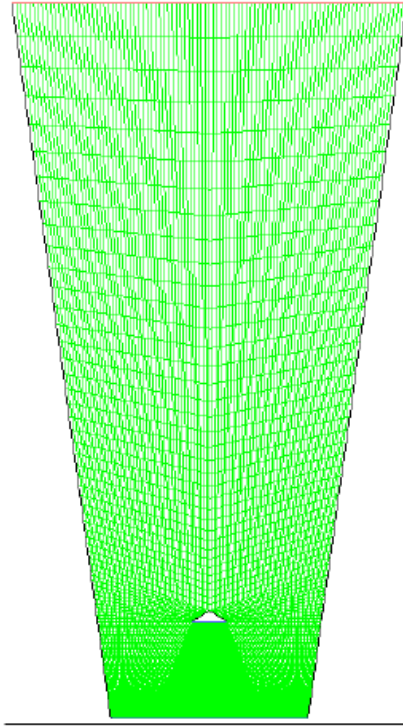


Figure2. Generated mesh for 2D-geometry

Momentum balance equation for solid phase is:

$$\frac{\partial}{\partial t}(\alpha_s \rho_s \vec{u}_s) + \nabla \cdot (\alpha_s \rho_s \vec{u}_s \vec{u}_s) = -\alpha_s \nabla P - \nabla P_s + \nabla \cdot \vec{\tau}_s + \alpha_s \rho_s g + \sum_{g=1}^n \beta_{gs} (\vec{u}_g - \vec{u}_s) \quad (3)$$

Momentum balance equation for gas phase is:

$$\frac{\partial}{\partial t}(\alpha_g \rho_g \vec{v}_g) + \nabla \cdot (\alpha_g \rho_g \vec{v}_g \vec{v}_g) = -\alpha_g \nabla P + \nabla \cdot \vec{\tau}_g + \sum_{g=1}^n \beta_{gs} (\vec{u}_g - \vec{u}_s) + \alpha_g \rho_g g \quad (4)$$

In momentum balance equation for solid phase, solid pressure and shear stress are obtained from the kinetic theory of granular flows which is established by Lun *et al.* [6]. Similar as thermodynamic temperature for gases, the granular temperature for solid particles is used to indicate particles velocity fluctuations and is described by equation (5):

$$\Theta_s = 1/3(v_s'^2) \quad (5)$$

The solid phase shear stress $\overline{\tau}_s$ is computed as follows:

$$\alpha_s \overline{\tau}_s = -P_s \overline{I} + \alpha_s \mu_s (\nabla u_s + (\nabla u_s)^T) + \alpha_s (\lambda_s - 2/3 \mu_s) \nabla u_s \quad (6)$$

where P_s is solid pressure, μ_s is solid shear viscosity and λ_s is solid bulk viscosity.

Solid pressure is computed by Lun's equation:

$$P_s = \alpha_s \rho_s \Theta_s + 2\rho_s (1 + e_{ss}) \alpha_s^2 g_{0,ss} \Theta_s \quad (7)$$

where e_{ss} is the coefficient of restitution for particle collisions with default value of 0.9 that indicates the particle's collision is close to elastic collision, $g_{0,ss}$ is the radial distribution function, and Θ_s is the granular temperature. The granular temperature is proportional to the kinetic energy of the fluctuating particle motion. The conservation equation for granular temperature is:

$$\frac{3}{2} \left[\frac{\partial}{\partial t} (\rho_s \alpha_s \Theta_s) + \nabla \cdot (\rho_s \alpha_s \Theta_s v_s) \right] = \left(-P_s \overline{I} + \overline{\tau}_s \right) : \nabla \overline{v}_s - \nabla \cdot (k_{\theta_s} \nabla \Theta_s) - \gamma_{\theta_s} \quad (8)$$

The term $\nabla \cdot (k_{\theta_s} \nabla \Theta_s)$ describing the diffusive flux of granular energy. The term γ_{θ_s} , represents the rate of energy dissipation within the solid phase due to collisions between particles.

$$\gamma_{\theta_s} = \frac{12(1 - e_{ss}^2) g_{0,ss}}{d_s \sqrt{\pi}} \alpha_s^2 \rho_s \Theta_s^{3/2} \quad (9)$$

Lun's equation for $g_{0,ss}$ is:

$$g_{0,ss} = \left[1 - \left(\frac{\alpha_s}{\alpha_{s,max}} \right) \right]^{-2.5 \alpha_{s,max}} \quad (10)$$

Solid shear viscosity is:

$$\mu_s = \mu_{s,col} + \mu_{s,kin} + \mu_{s,fric} \quad (11)$$

The frictional part of solid viscosity is only important when the solid volume fraction become close to solid packing limit ($\alpha_{s,max}$).

The contribution of collision in solid viscosity is:

$$\mu_{s,col} = \frac{4}{5} \alpha_s \rho_s d_s g_{0,ss} (1 + e_{ss}) \sqrt{\frac{\Theta_s}{\pi}} \quad (12)$$

The kinetic viscosity is computed in terms of Gidaspow's equation:

$$\mu_{s,kin} = \frac{10 d_s \rho_s \sqrt{\Theta_s \pi}}{96 \alpha_s (1 + e_{ss}) g_{0,ss}} \left[1 + \frac{4}{5} g_{0,ss} \alpha_s (1 + e_{ss}) \right]^2 \quad (13)$$

The bulk viscosity of solid phase is given by Lun's equation:

$$\lambda_s = 4/3 \alpha_s \rho_s d_p g_{0,ss} (1 + e_{ss}) \sqrt{\frac{\Theta_s}{\pi}} \quad (14)$$

The solids bulk viscosity accounts for the resistance of the granular particles to compression and expansion.

The interphase drag coefficient (β_{gs}) is calculated according to Gidaspow's equation:

$$\beta_{Ergun} = 150 \frac{\alpha_s^2 \mu_g}{\alpha_g d_s^2} + 1.75 \frac{\alpha_s \rho_g}{d_s} |v - u| \quad \alpha_g < 0.8 \quad (15)$$

$$\beta_{Wen-Yu} = 3/4 C_D \frac{\alpha_s \alpha_g \rho_g}{d_s} |v - u| \alpha_g^{-2.65}, \alpha_g \geq 0.8 \quad (16)$$

4. Turbulence model

The Realizable k- ϵ model is used to calculate turbulent terms of continuous gas phase. The term "Realizable" means that the model satisfies certain mathematical constraints on the Reynolds stresses, consistent with the physics of turbulent flows. An immediate benefit of the realizable k- ϵ model is that it more accurately predicts the spreading rate of both planar and round jets.

$$\frac{\partial}{\partial t} (\alpha_g \rho_g k_g) + \nabla \cdot (\alpha_g \rho_g k_g \overline{U}_g) = \nabla \cdot \left(\alpha_g \frac{\mu_{t,g}}{\sigma_k} \nabla k_g \right) - \alpha_g \rho_g \epsilon_g + \alpha_g \rho_g \Pi_{k,g} \quad (17)$$

$$\frac{\partial}{\partial t} (\alpha_g \rho_g \epsilon_g) + \nabla \cdot (\alpha_g \rho_g \epsilon_g \overline{U}_g) = \nabla \cdot \left(\alpha_g \frac{\mu_{t,g}}{\sigma_k} \nabla \epsilon_g \right) + \alpha_g \epsilon_g \left(\rho_g C_1 S - \rho_g C_2 \frac{\epsilon_g}{k_g + \sqrt{\nu_g \epsilon_g}} \right) + \alpha_g \rho_g \Pi_{\epsilon,g} \quad (18)$$

where σ_ϵ , σ_k are turbulent Prandtl number, $\Pi_{k,g}$ and $\Pi_{\epsilon,g}$ represent the influence of the dispersed phases on the continuous phase and $\mu_{t,g}$ is turbulent viscosity; k_g and ϵ_g are turbulent kinetic energy and dissipation rate respectively

$$C_1 = \max \left[0.43, \frac{\zeta}{\zeta + 5} \right] \quad (19)$$

$$\zeta = S \frac{k_g}{\epsilon_g} \quad (20)$$

$$S = \sqrt{2 E_{ij} E_{ij}} \quad (21)$$

$$C_2 = 1.9, \sigma_{\epsilon_g} = 1.2, \sigma_{k_g} = 1 \quad (22)$$

In dispersed turbulence model, interparticle collisions are negligible and the dominant process in the random motion of the secondary phases is the influence of the primary-phase turbulence.

Fluctuating quantities of the secondary phases can therefore be given in terms of the mean characteristics of the primary phase and the ratio of the particle relaxation time and eddy-particle interaction time.

The characteristic particle relaxation time connected with inertial effects acting on a dispersed phase S is defined as:

$$\tau_{F,Sg} = \alpha_g \rho_g \beta_{Sg}^{-1} \left(\frac{\rho_s}{\rho_g} + C_V \right) \quad (23)$$

The Lagrangian integral time scale calculated along particle trajectories, mainly affected by the crossing-trajectory effect, is defined as:

$$\tau_{t,Sg} = \frac{\tau_{t,g}}{\sqrt{1 + C_\beta \omega^2}} \quad (24)$$

$$\omega = \frac{|\vec{V}_{Sg}| \tau_{t,g}}{L_{t,g}} \quad (25)$$

$$C_\beta = 1.8 - 1.35 \cos^2 \theta \quad (26)$$

where θ is the angle between the mean particle velocity and the mean relative velocity. The ratio between these two characteristic times is written as:

$$\eta_{Sg} = \frac{\tau_{t,Sg}}{\tau_{F,Sg}} \quad (27)$$

The turbulence quantities for dispersed phase S are as follows:

$$k_S = k_g \left(\frac{b^2 + \eta_{Sg}}{1 + \eta_{Sg}} \right) \quad (28)$$

$$k_{Sg} = 2k_g \left(\frac{b + \eta_{Sg}}{1 + \eta_{Sg}} \right) \quad (29)$$

$$D_S = 1/3 k_{Sg} \tau_{t,Sg} \quad (30)$$

$$b = (1 + C_V) \left(\frac{\rho_S}{\rho_g} + C_V \right)^{-1} \quad (31)$$

D_S is the diffusion coefficient of solid particles and $C_V = 0.5$ is the added-mass coefficient.

5. Velocity distribution of outlet air from nozzle

As stated by various authors [6, 7, 8], the nozzle jet in a fluidized bed shows many similarities to a free axisymmetric jet, of which the gas velocity profiles are analogous to Schlichting *et al.* [10]. In Eqs. (32) and (33), \bar{r} is the dimensionless radial coordinate.

$$v_{at,ax}(h, \bar{r}) \sim \frac{1}{(h_{noz} - h)^{2/3}} \cdot \frac{1}{(1 + 0.25\bar{r}^2)} \quad (32)$$

$$v_{at,rd}(h, \bar{r}) \sim \frac{\bar{r} - 0.25\bar{r}^3}{(1 + 0.25\bar{r}^2)^2} \quad (33)$$

$$\bar{r} = \frac{2r}{r_{noz}(h)} \quad (34)$$

The jet radius produced by the pneumatic nozzle, $r_{noz}(h)$, is defined as the radius where the radial gas velocity, $v_{at,rd}(h, r)$, equals zero.

The jet velocity profiles which are produced by the pneumatic nozzle are depicted in figure3 and drawn numerically in figure4.

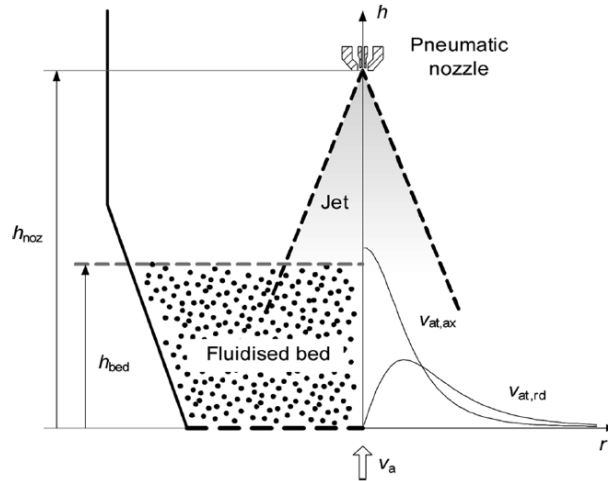


Fig. 3 The jet velocity profiles produced by the pneumatic nozzle as described by Schlichting *et al.* [9]

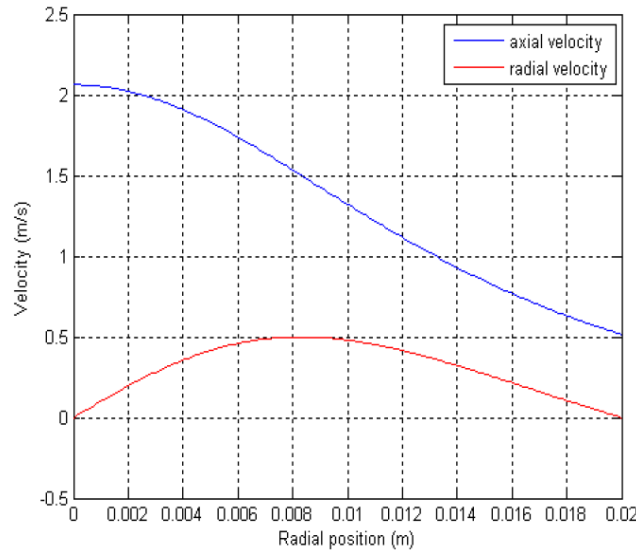


Figure 4 The jet velocity profiles (m/s)

6. Results and Discussion

The characteristics of the tapered bed are given in table2. The measured variables consist of the height of fluidized particles bed, temperature distribution and the relative humidity of air which has been reported [5]. In this study the height of fluidized particles bed is used for the validation of implemented hydrodynamic model.

According to Ronsse *et al.* [5], the height of fluidized particles bed is 0.93 m. the predicted height of fluidized particles which is average value over time, (figure 8) is in good agreement with the similar experimental measurement. The inlet gas in to tapered bed is air with mass flux of 1.371 (kg/m²s). The contours of mixture static pressure, particles velocity and gas velocity are depicted in figures 5a, 5b, 5c, respectively. Figure 5 shows, where the mixture static pressure decreases the particles and gas velocity increase. This result is consistent with the contours of particles volume fraction which is depicted in figure 8. In the region that air velocity increases, the particles volume fraction decreases. In figures 6,7 the velocity vectors of gas and solid particles are shown respectively. The turbulence of solid particles depends on the turbulent motion of gas phase this is evident through equations (28)-(31). At the bottom of bed there is high velocity of gas phase and maximum velocity fluctuations in this region leads to maximum turbulent motion of gas and solid phases. By increasing in the height of bed, the velocity and turbulence of gas phase decreases due to increasing in the diameter of bed hence, the drag force exerted on particles, by gas phase decreases and they fall down because of gravity force and the cycle is repeated again.

Table 2. Fluidized bed characteristics

Parameter	Value
Solid density (kg/m ³)	2600
Gas density (kg/m ³)	1.225
Gas viscosity (pa.s)	1.7894E-5
Particles diameter (μm)	365
Bed height (m)	0.84
Bottom diameter (m)	0.225
Top diameter (m)	0.45

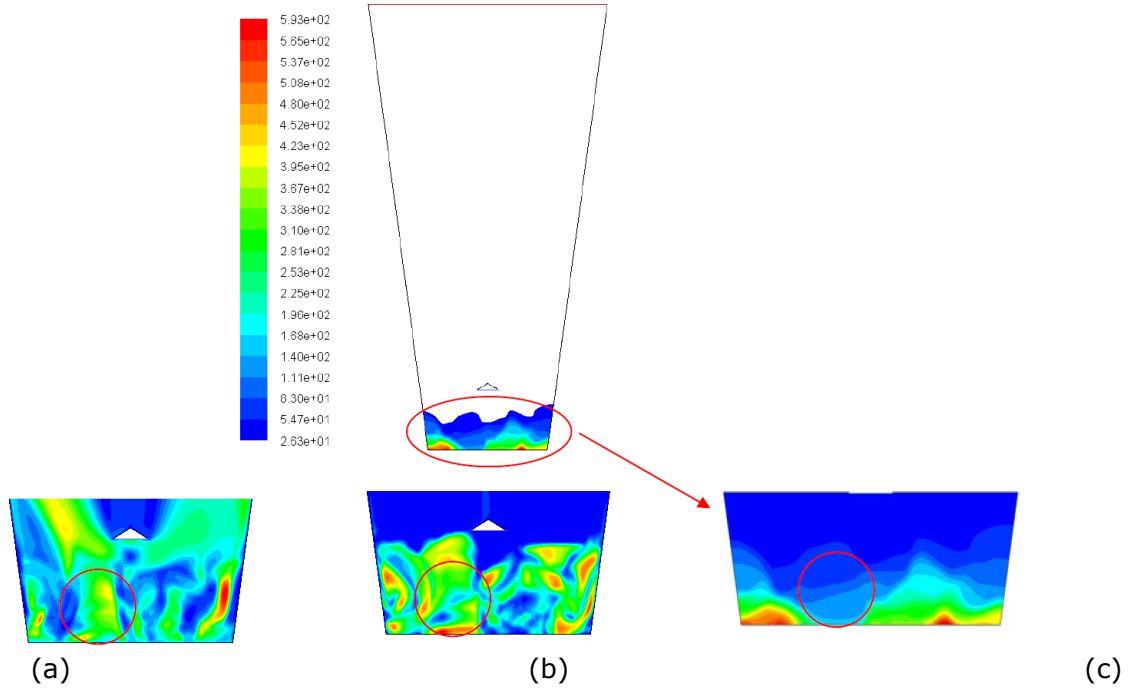


Figure 5 (a) Contours of gas velocity (m/s)-(b) contours of solid particle velocity (m/s)-(c) contours of mixture static gage pressure (Pa)

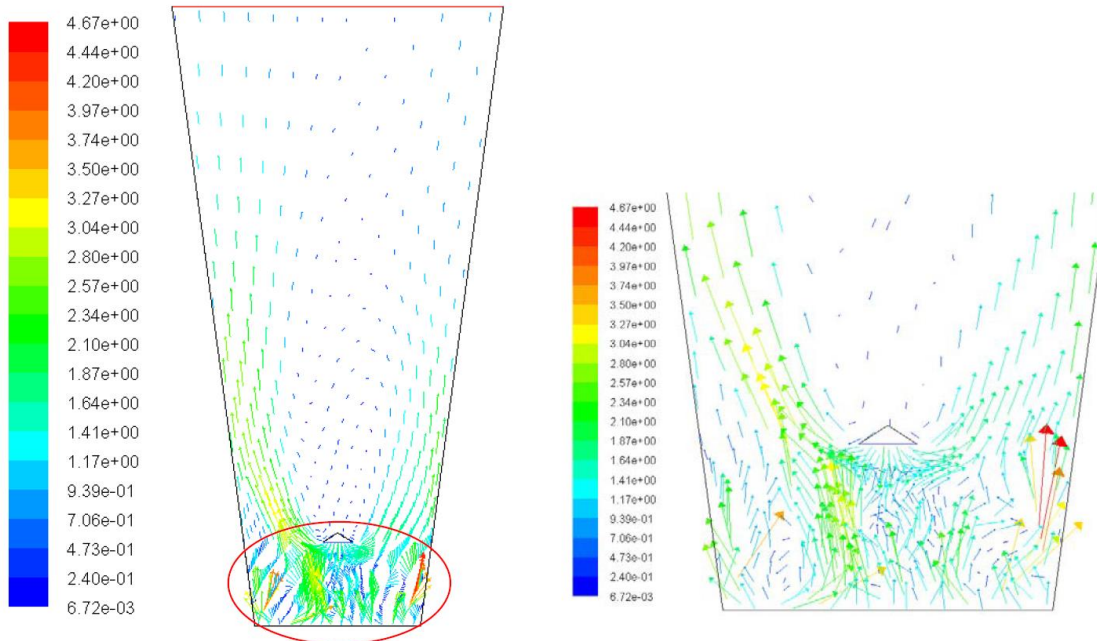


Figure 6 Velocity vectors of gas phase (m/s)

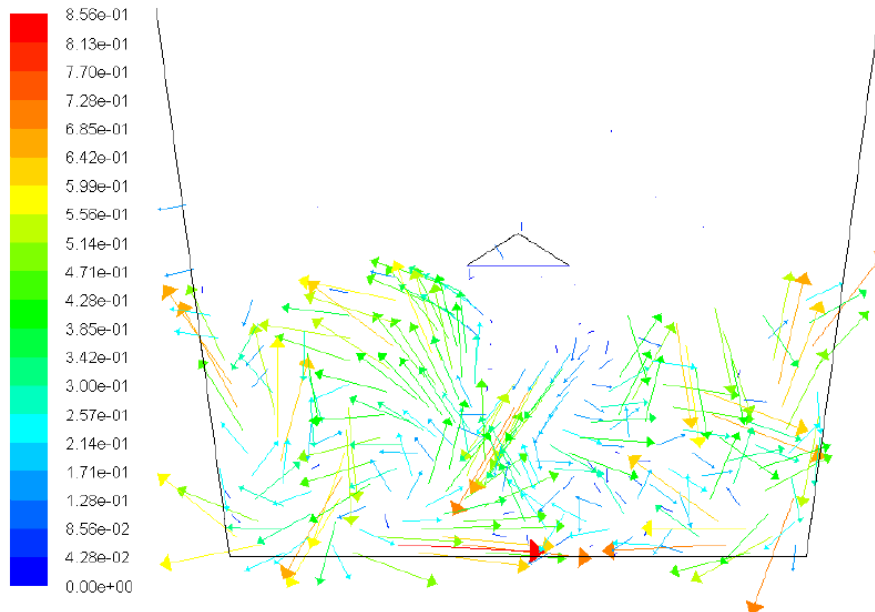


Figure 7 Velocity vectors of particles (m/s)

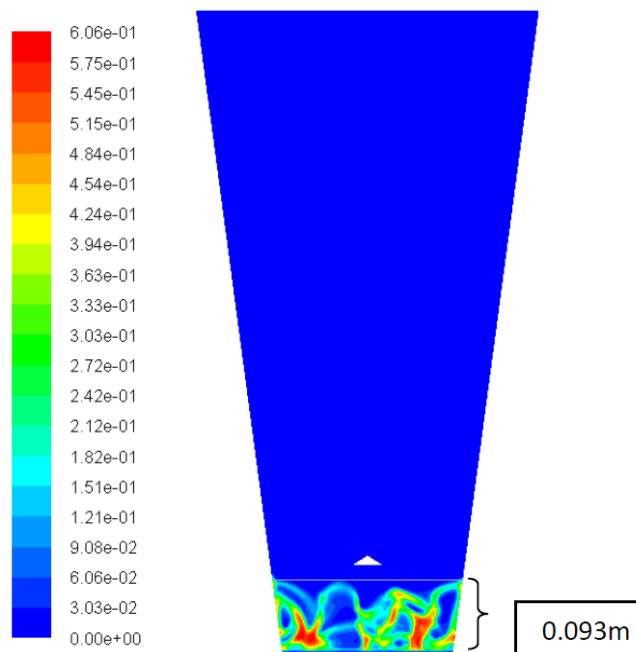


Figure 8 Contours of particles volume fraction

7. Conclusion

Although the products of coating process has vast applications in our life, there is a few information about processes (such as: droplet formation, evaporation over particles surface, droplet collision, heat transfer, hydrodynamic behavior of particles) occur in fluidized bed coating and how these processes affect the efficiency of coating. This is because there are a lot of variables influence fluidized bed coating. Therefore, it seems that trial and error is the only way to determine optimum operating conditions for fluidized bed coating. By utilizing modeling, one can investigate the effect of varies variables on fluidized bed coating process and decreases a need for huge amount of experimental analysis. Till now, diverse approaches are used for modeling fluidized bed coating, but, there is a lack of using CFD models. CFD models have advantage of being case independent. In other word, when CFD model is tuned in a range of operating conditions, the predictions of model for conditions out of this range

are more likely to be accurate in comparison with other models. Also, CFD model can evaluate for the effect of systems geometry (such as: design of baffle and inner pipe in fluidized bed) on coating efficiency [11].

In this study the CFD modeling of gas-solid flow in a 2D fluidized bed in Eulerian framework has been performed. The axial and radial velocity profiles of nozzles outlet air which is at the top of particles bed, has been simulated by means of Schlichting equation. The predicted height of particles fluidized bed is in good agreement with experimental measurement. This hydrodynamic modeling is initial step in CFD modeling of fluidized bed coating process.

References

- [1] Dewettinck, K., Huyghebaert, A.: Fluidized bed coating in food technology, *Food Science & Technology*, 10(1999) 163-168.
- [2] Werner, R. L. Stephen, Jones, R. Jim, Paterson, H. J. Anthony: Air suspension particle coating in the food industry: Part I- State of the art, *Pow. Tech.* 171(2007) 25-33.
- [3] Link, K.C. Schlünder, E.U.: Fluidized bed spray granulation. Investigation of the coating process on single sphere, *Chemical Engineering and Processing* 36 (1997) 443-457.
- [4] Polke, R., Schäfer, M.: Particle systems characterization as a fundamental element for process design and modeling, *Chemical Engineering Science* 57 (20) (2002) 4295-4299.
- [5] Ronsse, F., Pieters, G., Dewettinck, K.: Numerical spray model of the fluidized bed coating process, *Drying Tec.*, 25 (2007) 1491-1514.
- [6] Lun, C. K. K., Savage, S. B., Jeffrey, D. J., Chepurniy, N.: Kinetic Theories for Granular Flow: Inelastic Particles in Couette Flow and Slightly Inelastic Particles in a General Flow Field, *J. Fluid Mech.*, 140 (1984), 223-256.
- [7] Zank, J., Kind, M., Schlünder, E.U.: Particle growth and droplet deposition in fluidised bed granulation. *Powder Technology* 120 (1-2), (2001), 76-81.
- [8] Donadono, S., Mareca A., Massimilla, L.: Gas injection in shallow beds of fluidized, coarse solids. *Ingenieria Chimica Italiana*, 16, (1980), 1-10.
- [9] Becher, R.D., Schlünder, E.U.: Fluidized bed granulation: Gas flow, particle motion and moisture distribution. *Chemical Engineering and Processing*, 36 (4), (1997), 261-269.
- [10] Schlichting, H., Gersten, K., Krause, E., Oertel, H., Mayes, C.: *Boundary Layer Theory*, 8th Ed; Springer-Verlag: Berlin, (2004).
- [11] Turton, R.: Challenges in the modeling and prediction of coating of pharmaceutical dosage forms, *Pow. Tec.* (2007).